Crystal-field states of the Ce^{3+} ion in CeF_3: A demonstration of vibronic interaction in ionic rare-earth compounds

H. Gerlinger* and G. Schaack
Physikalisches Institut der Universität Würzburg, Röntgenring 8, D-8700 Würzburg, Federal Republic of Germany
(Received 31 October 1985; revised manuscript received 21 January 1986)

We have investigated the Raman, infrared, and EPR spectra of CeF_3 in a search for the excited crystal-field levels of the $4f^1$ configuration in this compound. While this can be achieved routinely for the $^2F_{7/2}$ levels between 2100 and 2900 cm^{-1}, problems arise for the $^2F_{5/2}$ levels because of a strong interaction between the electronic states and the near-resonant optical phonons. Pure electronic crystal-field states obviously do not exist in this range, but are hybridized with optical phonons and additional, new vibronic states are found in the wave-number regions of the expected crystal-field levels. A tentative model of a local Jahn-Teller—type $4f$-electron—phonon interaction is studied, but only qualitative agreement with the experimental results can be obtained. Approximate values for the wave numbers of the uncoupled crystal-field states are given. An extrapolation of existing values of crystal-field parameters for the trigonal tysonite structure to CeF_3 gives reasonable agreement between calculated crystal-field levels and the findings from experiment for these uncoupled states.

I. INTRODUCTION

The rare-earth trifluorides [RF_3, (D_{3d}^4,$P\bar{3}c1$)] in the tysonite structure have been investigated carefully in the past in many different species. LaF_3, for example, is an excellent ionic conductor at elevated temperatures[1] and the good transmission properties in the ultraviolet of this host material for rare-earth (R) dopants has permitted laser activity in the vuv (LaF_3:Nd^{3+},$\lambda = 1720$ Å).[2] Several attempts have been made to calculate the crystal-field energies and eigenfunctions of electronic levels of R^{3+} ions in these hosts, especially in LaF_3, and to determine the crystal-field parameters using models of various degrees of sophistication.

Whereas parameter fits for Pr^{3+} and the heavier R^{3+} ions can be performed routinely with good success because of the detailed knowledge about the many electronic levels in the crystalline Stark field, there exist several difficulties which impede such a straightforward analysis for CeF_3:

Both Raman and far-infrared (FIR) experiments demonstrate several effects, due to an unusually strong $4f$-electron—optical-phonon interaction[3,4] in the region of the $^2F_{5/2}$ state [magnetoelastic (me) and vibronic interaction] resulting in a hybridization of $4f$ states with nearby phonon states. Effects of the me interaction are characterized by temperature-dependent energy shifts of phononlike states or a splitting of degenerate phonon states $\Delta\bar{\nu}$ in a magnetic field B. These effects saturate at high fields and low temperatures, according to the paramagnetic saturation of the twofold-degenerate electronic ground state:

$$\Delta\bar{\nu} \propto \tanh(g\mu_B B/k_B T) , \quad (1)$$

with the observed g factor of the ground state. Such nonlinear magnetic shifts and splittings of phononlike states are found in the spectra of CeF_3 for several transitions.[3,4] The vibronic interaction manifests itself by $4f$-electron—phonon anticrossing phenomena and gives rise to additional "vibronic" states and transitions in the spectra.

The energy shifts of the observed electronic states due to this interaction, i.e., the shifts of the actual hybridized levels as compared to the hypothetical uncoupled states, which have to be used in the crystal-field analysis, may amount to about 30 cm^{-1}, or even more. These shifts, which cannot be determined precisely, add a new source of uncertainty to the crystal-field analysis. Moreover, the usual classification of a spectroscopically observed state as either a crystal-field excitation or a phonon, almost self-evident for a $4f$ spectroscopist, is no longer justified, but the vibronic states[5,3] blur the spectra by additional structure, which may cause some arbitrariness in the identification of those vibronic transitions, where the electronic character prevails. Such additional vibronic states always arise whenever the electronic ground state is degenerate and the interaction strength is adequate. It should be realized that the term "vibronic state" or "vibronic transition" is used here not for phonon-sidebands, where a phonon and an electronic excitation are excited simultaneously by one photon,[6] but for states, whose wave functions are linear combinations of Born-Oppenheimer products as in treatments of the static or dynamic Jahn-Teller effect (e.g., Ref. 7).

When the energies of the uncoupled excited crystal-field states have been deduced from the spectra, another problem arises, as only one multiplet ^2F exists in the $4f^1$ configuration with the two components $J = \frac{5}{2}$ and $\frac{7}{2}$. In a crystal field of a symmetry lower than cubic, the $^2F_{5/2}$ component is split into three crystal-field states and the $^2F_{7/2}$ component is split into four crystal-field states, each doubly (Kramers) degenerate. For the C_2-site symmetry in the tysonite lattice, theory postulates 14 independent

crystal-field parameters, whereas only five Stark splittings are provided by experiment. Thus the usual parametrization and fit procedure is not applicable here.

In the past, several attempts were made to determine crystal-field parameters of Ce^{3+} in this lattice. Already in 1934, van Vleck and Hebb[8] tried, in a paper, which marked the very beginning of crystal-field theory, to derive the crystal-field energies and the eigenfunctions of the $^2F_{5/2}$ component from Faraday-rotation experiments in natural tysonite by Becquerel and de Haas.[9] They assumed rhombic site symmetry with the axis of quantization oriented parallel to the principal crystallographic axis Z.

Baker and Rubins[10] observed, by EPR, the axes of the local g tensors. One Cartesian axis, chosen to be the y axis, lies in the basal plane parallel to a twofold axis of the crystal, the other two local axes are oriented in a plane comprising the optical axis $\hat{\mathbf{Z}}$; the local z' axis, the quantization axis, is assumed to make an angle θ with $\hat{\mathbf{Z}}$, θ varies with the type of R ion considered. The wave functions of the ground states have been calculated from these results.

In the most recent work on this subject, Morrison and Leavitt[11] extrapolated their fit results for the R^{3+} ($Pr^{3+}, \ldots, Tm^{3+}$) in LaF_3 to the case of Ce^{3+} in this host. No experimental data of Ce^{3+} in LaF_3 are considered in this investigation. Their calculations are based on the assumption of a C_2-site symmetry for the R ions with the quantization axis perpendicular to $\hat{\mathbf{Z}}$. Calculations with the approximate site symmetry D_{3h} for the odd-electron systems are also available, and only four crystal-field parameters are required in this case.[12]

The correct symmetry of the tysonite lattice has been the subject of controversial discussion over decades (see Ref. 13 for a review of the early work). Only recently has this question been settled in favor of the microtwinned trigonal D^4_{3d} ($P\bar{3}c1$) structure[14–16] instead of the hexagonal C^3_{6v} ($P6_3cm$) or any other structure.[17] The site symmetry of the R ions is C_2 with the quantization axis oriented perpendicular to C_3, and there are six formula units per unit cell.

II. EXPERIMENTAL RESULTS

Three different techniques were used in this work to study the transitions between the vibronic states in CeF_3: Raman spectroscopy, infrared reflection spectroscopy, and EPR. In all cases, the samples were cooled by immersion in superfluid helium ($T \approx 2$ K). The spectra were taken in external magnetic fields B up to 8 T using a split-coil superconducting solenoid or up to 12 T in a Bitter coil. The Raman spectra were excited with an Ar^+ laser (5145 Å) and analyzed using standard techniques with a resolution of 2.5 cm^{-1}. The infrared spectra of circularly shaped (1-cm diam) and oriented probes were studied in the wave-number region $30 \leq \bar{\nu} \leq 600$ cm^{-1}, using the Fourier technique in both the Faraday and Voigt configurations ($\mathbf{B} \| \hat{\mathbf{Z}} \| \mathbf{k}$ or $\mathbf{B} \| \hat{\mathbf{Z}} \perp \mathbf{k}$, respectively; k is the wave vector of the incident radiation). For the evaluation of the reflectivity data, we performed a Kramers-Kronig analysis and, for refinement, a Lorentzian oscillator fit,[4] using the results of the KK analysis as starting values. The EPR spectra were taken in a superconducting magnet ($B \leq 9$ T) using a transmission geometry.[18] The frequencies in the W band (about 80 GHz) and harmonics thereof were generated by an IMPATT diode.

The transitions to the $^2F_{7/2}$ states were already investigated by infrared transmission by Buchanan *et al.*[19] We verified their results by means of Raman spectroscopy. The crystals purchased from OPTOVAC Inc. (North Brookfield, Massachusetts) were oriented using cleavage planes and x-ray backscattering, and the surfaces were optically polished.

Figure 1 (lower part) interrelates the crystal coordinates (X,Y,Z) with the local systems (x,y,z) of three RE ions, at $Z = \frac{1}{4}$ or $\frac{3}{4}$; the inset gives the orientation of the Cartesian axes of the g tensors. All data of the g factors are related to the system of local coordinates.

The g factors of the electronic ground state, where the vibronic character can be ignored to a good approximation, have been determined for LaF_3(0.3 at.% Ce^{3+}) in Ref. 10; these values together with our results for CeF_3 are compiled in Table I. In Fig. 2, the Raman transitions to the excited Kramers component of the ground state are shown for $\mathbf{B} \| \hat{\mathbf{Z}}$ and $\mathbf{B} \perp \hat{\mathbf{Z}}$. The spectrum $\mathbf{B} \perp \hat{\mathbf{Z}}$ has been numerically decomposed into three components of identical strength in accordance with the inclination of the field direction of 80° against one of the three C_2 axes in the basal plane. The angle θ (Fig. 1) has been determined in Ref. 10: $\theta_1 = 14°$; we have obtained the same value in concentrated CeF_3. For the excited states, $\theta_{2,3}$ have not been determined, as the reduced experimental accuracy for these states does not justify this.

Figures 3 and 4 give the E_u reststrahlen spectra of CeF_3 at different magnetic fields $\mathbf{B} \| \hat{\mathbf{Z}}$ in the Faraday (Fig. 3) and Voigt configurations (Fig. 4). The spectra at $B = 0$ are identical in both configurations and agree well with

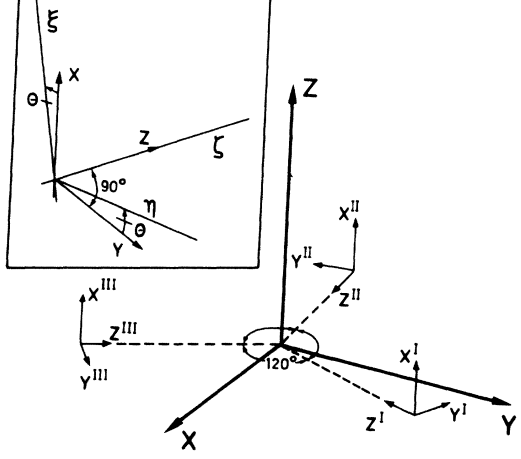

FIG. 1. Coordinate system XYZ of the crystal ($\hat{\mathbf{Z}} \| C_3 \| \mathbf{B}$) and local coordinate systems of three R ions in RF_3; z^i is the local axis of quantization. The inset shows the local system and the axes of the g tensor.

TABLE I. Experimental g factors and energies $\bar{\nu}$ of those vibronic states derived from $^2F_{5/2}$ in CeF_3 which demonstrate a linear Zeeman effect. Wave numbers in parentheses are experimental values extrapolated to $B=0$ T; other values are the calculated results for the uncoupled states.

	Baker *et al.*[a] ($La_{1-x}Ce_xF_3$; $x=0.003$)	Raman g	$\bar{\nu}$ (cm^{-1})	EPR and IR g	$\bar{\nu}$ (cm^{-1})
$g_{x,I}$	1.304	1.25		1.3[b]	
$g_{y,I}$	0.16	0.38	0	0.42[b]	0
$g_{z,I}$	0.45	0.47		0.48[b]	
$g_{x,II}$		0.45	(142.6)[d]	0.5[c]	(153) ≈ 160
$g_{x,III}$				0.25[c]	(258)
$g_{y,III}$			≈ 290[d]	(0.5)[c]	≈ 280
$g_{z,III}$				(0.5)[c]	

[a]Reference 10.
[b]EPR.
[c]IR (infrared).
[d]Reference 3.

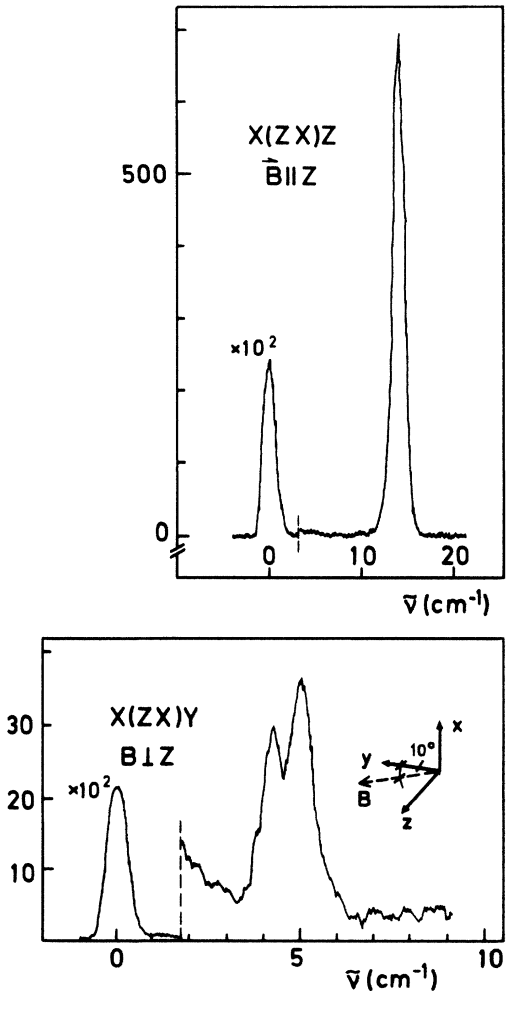

FIG. 2. Raman spectra (counts per second, cps) of transitions within the Kramers degenerate ground state of CeF_3, $B=12$ T; spectral slit-width: 1.5 cm^{-1} ($\mathbf{B}||\hat{\mathbf{Z}}$), 0.8 cm^{-1} ($\mathbf{B}\perp\hat{\mathbf{Z}}$). The inclination of the **B** direction against one of the local y axes is indicated; $T=2$ K.

the spectra taken by Lowndes *et al.*,[20] but characteristic differences develop with increasing B.[4] These differences and the general B dependence of the spectra will be treated in detail elsewhere.[21] In this reference, all phonon frequencies and frequencies of vibronic states of CeF_3 taken from Raman and FIR spectra will be compiled and compared with the spectra of isomorphous LaF_3. In summarizing, we find that almost every band shifts nonlinearly

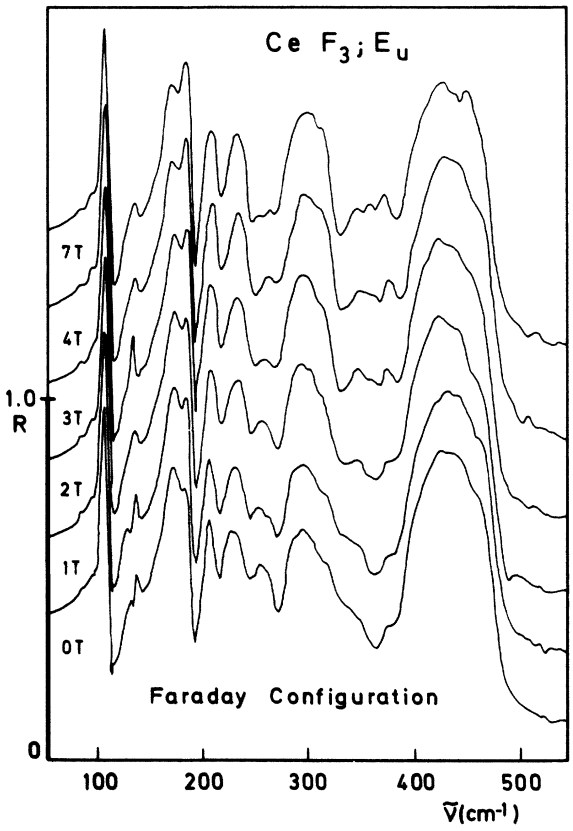

FIG. 3. Magnetic field (B) dependence of FIR reflectivity R of CeF_3, $\mathbf{E}\perp\hat{\mathbf{Z}}$, $T=1.8$ K; $\mathbf{B}||\hat{\mathbf{Z}}||\mathbf{k}$ ($\mathbf{k}$ is wave vector of incident radiation with electric vector **E**), E_u symmetry.

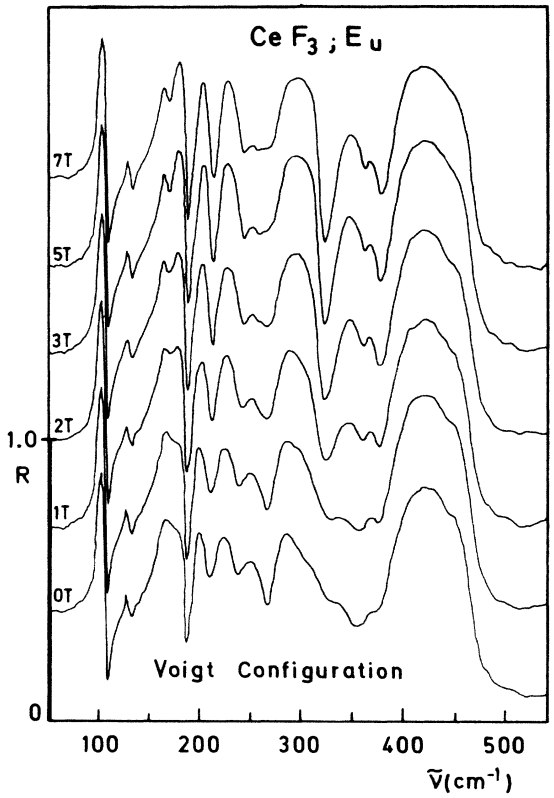

FIG. 4. B dependence of FIR reflectivity R of CeF_3, $\mathbf{E}\perp\hat{\mathbf{Z}}$, $T=1.8$ K; $\mathbf{B}\|\hat{\mathbf{Z}}\perp\mathbf{k}$, E_u symmetry.

with B by small amounts (<5 cm^{-1}) following Eq. (1), i.e., there is a linear shift at small fields which saturates at about 3 T for $T\approx 2$ K. In Fig. 5, the A_{2u} reststrahlen spectra are depicted under a magnetic field $\mathbf{B}\|\hat{\mathbf{Z}}$ and similar shifts are found in these spectra.[21]

The Raman spectra of CeF_3 (Fig. 6) of E type

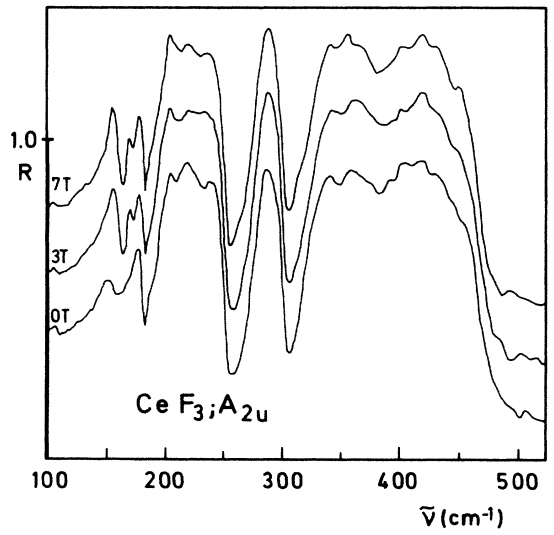

FIG. 5. $R(B)$ of CeF_3, $\mathbf{E}\|\hat{\mathbf{Z}}$, $T=1.8$ K; $\mathbf{B}\|\hat{\mathbf{Z}}\perp\mathbf{k}$, A_{2u} symmetry.

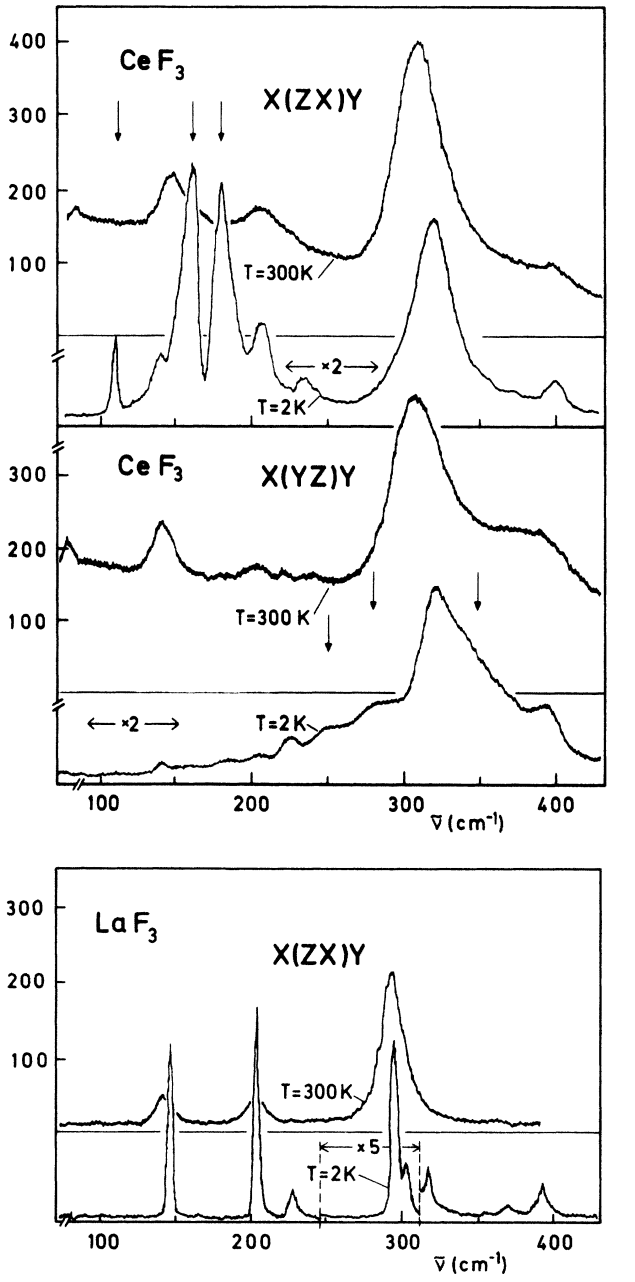

FIG. 6. Raman spectra (cps) of CeF_3 and isomorphous LaF_3, $T=2$ K and $T=300$ K; E_g type [E_{1g} in the approximate D_{6h} symmetry (Ref. 13)]. The antisymmetry in the spectra of the Ce^{3+} compound ($T=2$ K) is evident, the transitions marked by arrows are due to additional vibronic states as discussed in the text, and the unmarked bands are phonon transitions. The $X(YZ)Y$ spectra of LaF_3 are identical with the $X(ZX)Y$ spectra shown.

[$X(YX)Y$ and $X(ZX)Y$ geometry] have been discussed in Ref. 3. Both types of Raman spectra are governed by the strong "phonon" bands and additional vibronic features, which are responsible for the striking antisymmetric scattering [$(ZX)\neq(YZ)$] appearing in Fig. 6. If only phonons were excited, both spectra in Fig. 6 should be identical, as observed in diamagnetic LaF_3, where Placzek's polarizability theory applies. Antisymmetric scattering

occurs whenever the scattering tensor comprises terms, which transform like a pseudovector,[22] beside the usual symmetric contributions. This situation is, for example, encountered for scattering processes between levels transforming according to the irreducible representations (ir) of the double groups, i.e., between Kramers degenerate levels of electronic or vibronic origin. Raman transitions in CeF_3, where antisymmetric scattering prevails, are indicated by arrows in Fig. 6. They are found around 150 cm^{-1} and around 300 cm^{-1}. These transitions must be of vibronic origin, as only two pure electronic transitions should be expected within $^2F_{5/2}$, Raman spectra of CeF_3 taken at higher temperature are approaching symmetry and are in good agreement with the spectra reported in Ref. 13. Transitions of essentially electronic character are not easily detectable, but should be revealed by careful study of the B dependence of the spectra, searching for details exhibiting an approximately linear Zeeman effect. This linear Zeeman effect may, however, be disturbed by anticrossing effects with nearby vibronic bands, as shown in Fig. 7. In this figure, a section of the Raman spectrum of E_g symmetry of CeF_3 is depicted. The feature at 150 cm^{-1}, emerging at high magnetic fields, performs a linear Zeeman shift [Fig. 8(a)] after numerical decoupling (e.g., Ref. 23) from the vibronic transition at 153 cm^{-1}, starting at $\bar{\nu}=142.6$ cm^{-1} ($B=0$). This anticrossing is further testified by an exchange of transition intensities between the two coupled states, due to their hybridization [Fig. 8(b)]. Taking into account the g factor of the ground state (Table I), a g factor for the excited level,

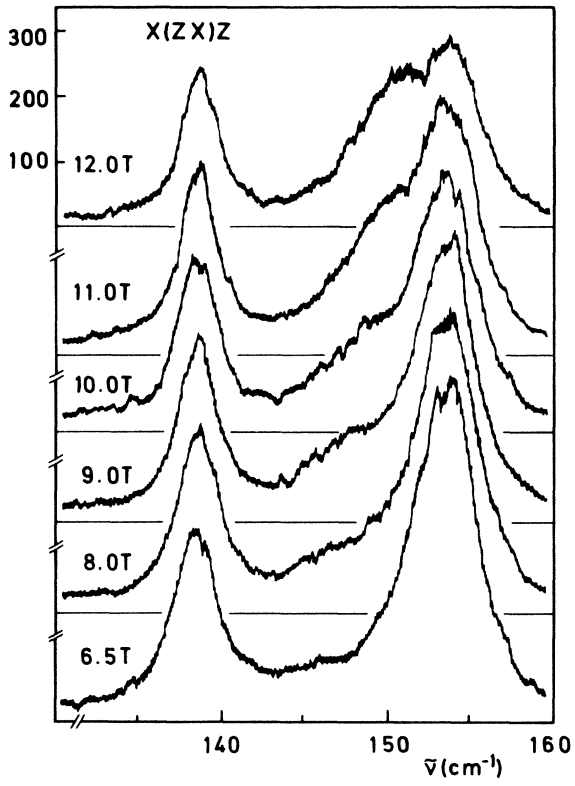

FIG. 7. Anticrossing behavior in the Raman spectra (cps) of two vibronic states in CeF_3, $T=2$ K, $\mathbf{B}||\hat{\mathbf{Z}}$.

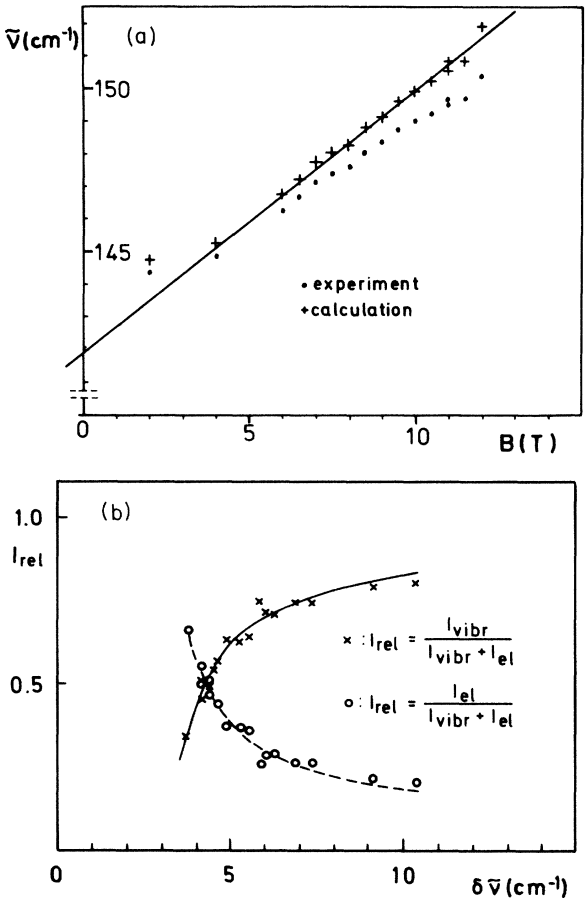

FIG. 8. (a) Results of a numerical decoupling (Ref. 23) of the two transitions shown in Fig. 7. Experiment: wave numbers of the strongly-field-dependent component as taken from Fig. 7; accuracy: ± 1 cm^{-1}, ±2 cm^{-1} at low fields; calculation: result of the numerical decoupling. (b) Normalized transition intensities I_{rel} of the coupled transitions as a function of the energy differences $\delta\bar{\nu}$ of the decoupled states; vibr. denotes vibronic line at 155.5 cm^{-1}, el denotes quasielectronic line of (a). The solid and dashed lines are the results of calculations.

$g_{x,II}=0.45$, is derived. This Raman transition obviously ends in the upper Kramers component of the first-excited crystal-field state.

On the other hand, the FIR experiments yield another, almost linearly shifting band starting at 153.5 cm^{-1} ($B=0$) in the A_{2u} spectrum (Figs. 5 and 9). Here a g factor $g_{x,II}=0.5$ is obtained; the transition leads to the lower Kramers component of the excited state. Buchanan *et al.*[19] observed two broad electronic "hot absorption lines" ($T=77$ K), which were attributed to transitions to the $^2F_{7/2}$ manifold starting from an excited crystal-field state at 150 cm^{-1}. Van Vleck and Hebb[8] calculated this level at 130 cm^{-1}. Considering our spectroscopic results, the situation appears quite complicated: The first-excited crystal-field component is not a single state, but may have decayed into several separate vibronic states with a complicated magnetic field dependence. A detailed spectroscopic analysis of these vibronic states will be presented in

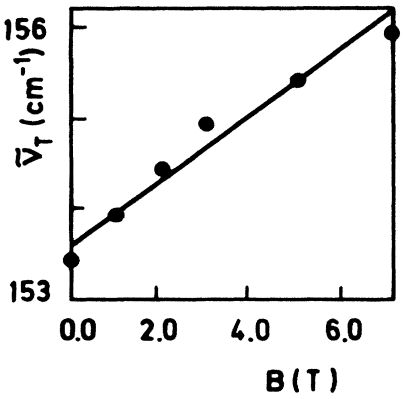

FIG. 9. Magnetic field dependence of the transverse frequency of an A_{2u} oscillator in CeF_3, $\mathbf{B}||\hat{\mathbf{Z}}$, $T=2$ K.

a separate paper,[24] where the frequencies of these vibronic states and their magnetic field temperature, and concentration (c in $Ce_cLa_{1-c}F_3$) dependences will be compiled. As an example, Fig. 10 shows the B dependence of the energy of three vibronic states ($2E_g$, $1A_g$). These results can be summarized by saying that at low temperatures in a magnetic field, these states follow roughly (1) (see also Sec. III below), and that the splitting between different vibronic levels and the intensities of the transitions generally disappear with decreasing concentration c and with increasing temperature. This latter tendency is indicated in Fig. 6. The frequencies of vibronic transitions with A_g symmetry do not generally coincide with E_g transitions. As a consequence, we expect the uncoupled first-excited crystal-field level in the region $140<\bar{\nu}<170$ cm^{-1}. A very recent investigation[25] of the magnetization and of the specific heat of CeF_3 at $4.2\leq T\leq 300$ K locates this first-excited level at 75 cm^{-1}. This finding is not supported by spectroscopic results.

The second-excited crystal-field level again could not be traced directly in the Raman spectra up to 1000 cm^{-1}. The only indication of the presence of this second level is another accumulation of new vibronic states near 300 cm^{-1} (Fig. 6) similar to the vibronic states near 150 cm^{-1} and a magnetic-field-dependent change of a phonon band shape (Fig. 11), which continues to the highest field attainable, contrary to the usual magnetoelastic effects in the Raman spectra,[3] which saturate according to (1).

In the FIR spectra both in the Voigt and Faraday configurations, a weak reflection band near 258 cm^{-1} is found with an approximately linear shift to higher wave numbers in an external magnetic field (Fig. 12). The g factor of this state is found to be $g_x=0.25$, after subtracting the effect of the ground state. Thus the missing level is to be expected in the wave-number region between 250 and 320 cm^{-1}. In Ref. 8, the second electronic level of $^2F_{5/2}$ was calculated at 750 cm^{-1}; in Ref. 19, it was assumed to lie close to 500 cm^{-1}.

The situation is much simpler for the transitions to the $^2F_{7/2}$ component, which lie outside the region of lattice excitations and where no me effects interfere. We have observed these transitions by means of Raman scattering and have observed the following Raman transitions to the four crystal-field components of $^2F_{7/2}$: 2161, 2239, 2640, and 2860 cm^{-1}, which agree, within experimental accuracy, with the results obtained by Buchanan *et al.*[19] using infrared spectroscopy. A Zeeman splitting was observed only for the lowest state at 2161 cm^{-1}; $g_x=1.65$. The other transitions are presumably too broad to observe an

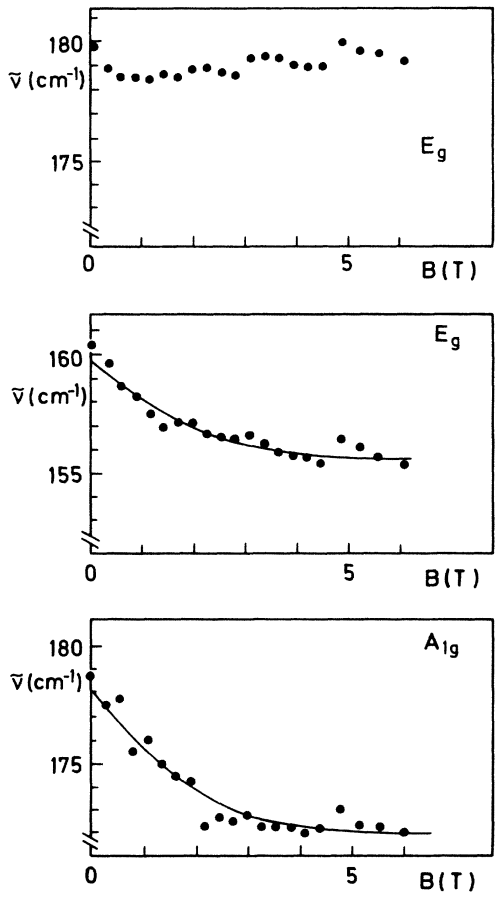

FIG. 10. Magnetic field dependence of Raman-active vibronic transitions of different ir's; the E_g transitions plotted here are the two prominent bands indicated in Fig. 6 [$X(ZX)Y$].

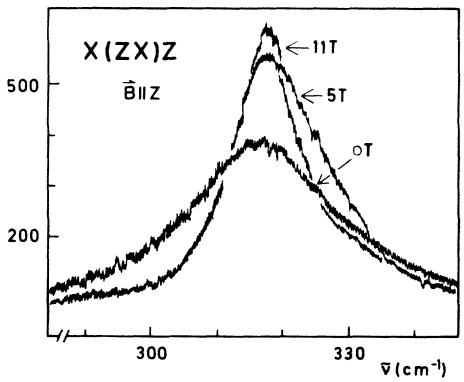

FIG. 11. Field-dependent Raman band shape (cps) of a phononlike vibronic transition in CeF_3, $T=2$ K, $\mathbf{B}||\hat{\mathbf{Z}}$.

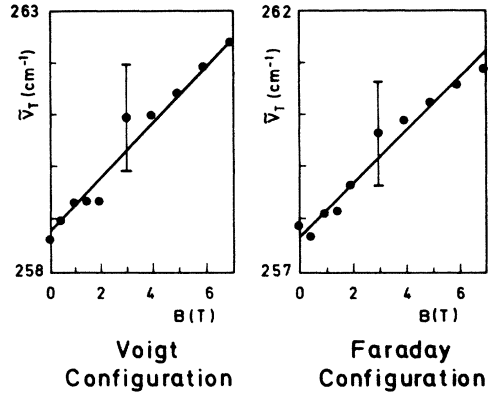

FIG. 12. Field-dependent transverse E_u oscillator in CeF_3, $\mathbf{B}||\hat{\mathbf{Z}}$, $T=2$ K, in the Voigt and Faraday configurations.

effect of a magnetic field. Except for fluorescence lines occuring in the Raman spectra in this region, possibly due to other R impurities, no ambiguities were encountered in attributing the transitions and also no line multiplication. This gives strong evidence that the $4f^1$-electron–phonon coupling is, in fact, the main source of the effects described above.

All the experimental facts mentioned above are certainly not due to magnetic or electric multipolar ordering, but all occur in the paramagnetic state of CeF_3. Recent measurements of the specific heat c_p of CeF_3 (Ref. 26) have revealed two anomalies of $c_p(B=0)$ peaking at 0.4 and 0.12 K, respectively. Thus an ordered state may exist only in the millikelvin region.

III. DISCUSSION

In this section, we discuss a simple model of vibronic states in CeF_3, which is based on a theory of Thalmeier and Fulde[5] originally developed for similar effects in the Laves-phase intermetallic compound $CeAl_2$. Our model interprets the energy levels of a single Ce^{3+} ion interacting with the local optical-phonon modes of its surrounding ligands.

Without me interaction the states of the system of $4f^1$ electrons and local modes are Born-Oppenheimer states, products of electronic and vibrational states:

$$|\bar{\Psi}(\omega_i^{np})\rangle = |\Psi_{\rm el}^n\rangle\,|p(\hbar\omega_i)\rangle\ , \tag{2}$$

where the electronic component is n-fold degenerate and the phonon state is p-fold occupied with phonons of energy $\hbar\omega_i$. The coupling is governed by the usual bilinear Jahn-Teller Hamiltonian:

$$H_{\rm me}=\sum_{i,\Gamma,\Gamma'} G_{kq,i}^{\Gamma,\Gamma'} C_{kq}^{\Gamma'} \phi_i^{\Gamma}\ . \tag{3}$$

Here, ϕ_i^{Γ} is a phonon operator of mode i, and symmetry type Γ, $C_{kq}^{\Gamma'}$ is an electronic multipole operator of rank k ($k=2,4,6$) and order q ($-k\le q\le k$), transforming according to the ir Γ', as generally used in crystal-field theory. G is a coupling constant, the dynamical crystal-field parameter,[27] which can, in favorable cases, be determined by fitting of experimental results. In (3), no summation on the R ions per unit cell is performed as the interaction is completely local in this context. Another approximation of the Thalmeier-Fulde model is the reduction of the product space (2) to those states, with energies close to resonance. We only consider product states of single phonons with the electronic ground state and products of zero-phonon states with the excited electronic state. On the contrary, in the usual treatment of the me interaction, which considers the same type of Hamiltonian (3), just the off-resonance case is considered,[28,3,27] and many-particle techniques are used corresponding to a second-order perturbation theory. In the present case, however, the Hamiltonian is diagonalized in a restricted basis of states.

The ir of the vibronic and the electronic states are those of the double group[29] of $C_2(\Gamma_3,\Gamma_4)$ because

$$\Gamma_1\otimes\Gamma_{3,4}=\Gamma_{3,4},\quad \Gamma_2\otimes\Gamma_{3,4}=\Gamma_{4,3}\ .$$

As $\Gamma_3\otimes\Gamma_4=\Gamma_1$ and $\Gamma_{3,4}\otimes\Gamma_{3,4}=\Gamma_2$, all polarizations are allowed for transitions between the degenerate vibronic states.[22] As a consequence of this, vibronically coupled E phonons will produce additional transitions in the A spectra and vibronic transitions will simultaneously occur both in the infrared and Raman spectra, because the inversion center of D_{3d} is ineffective in this local model with site symmetry C_2.

For the sake of simplicity, we restrict the calculations to electronic operators of rank $k=2$ (quadrupoles). Recent studies[27] for the compound $LiTbF_4$ have shown that this is a crude approximation as at least the operators for $k=4$ contribute as strongly as the quadrupoles to vibronic and magnetoelastic effects, but will provide no qualitatively new results. The quadrupole operators can be written in tensorial form:

$$Q_{ij}=\int (3x_ix_j-r^2\delta_{ij})\rho_{4f}(x)d^3x\ ,$$
$$i,j=1,2,3,\ r^2=\sum_i x_i^2\ .$$

The matrix elements are evaluated as usual using Stevens's operator equivalence:

$$\begin{aligned}
&Q_{13}\propto J_xJ_z+J_zJ_x=O_1\quad(\Gamma_2)\ ,\\
&\tfrac{1}{3}(Q_{11}-Q_{22})\propto J_xJ_x-J_yJ_y=O_2\quad(\Gamma_1)\ ,\\
&Q_{23}\propto J_yJ_z+J_zJ_y=O_3\quad(\Gamma_2)\ ,\\
&Q_{12}\propto J_xJ_y+J_yJ_x=O_4\quad(\Gamma_1)\ ,\\
&Q_{33}\propto 3J_z^2-J^2=O_5\quad(\Gamma_1)\ .
\end{aligned} \tag{4}$$

The interaction Hamiltonian (3) is now reformulated:

$$H=\sum_{i,j} G_{ij}O_j\phi_i\ . \tag{5}$$

We consider for the model calculation one E phonon in D_{3d} with energy ω, with its components P_1,P_2 transforming locally according to Γ_1 and Γ_2, coupled with an excited electronic Kramers degenerate level $E_{i\pm}$ of wave number $\bar{\nu}_i$ (ground state $\bar{\nu}_0$). We obtain the already block-diagonalized matrix:

$$
\begin{array}{c|cccccc}
 & |E_{i+},0\rangle & |E_{0-},P_2\rangle & |E_{0+},P_1\rangle & |E_{0-},P_1\rangle & |E_{0+},P_2\rangle & |E_{i-},0\rangle \\
\hline
\langle 0,E_{i+}| & \bar{\nu}_i & M_B & M_A & 0 & 0 & 0 \\
\langle P_2,E_{0-}| & M_B^* & \omega & 0 & 0 & 0 & 0 \\
\langle P_1,E_{0+}| & M_A^* & 0 & \omega & 0 & 0 & 0 \\
\langle P_1,E_{0-}| & 0 & 0 & 0 & \omega & 0 & M_A \\
\langle P_2,E_{0+}| & 0 & 0 & 0 & 0 & \omega & M_B \\
\langle 0,E_{i-}| & 0 & 0 & 0 & M_A^* & M_B^* & \bar{\nu}_i
\end{array}
\tag{6}
$$

The matrix elements are defined as

$$
\begin{aligned}
M_A &= \langle O,E_{i\pm}| \sum_{j=2,4,5} G_{j,1} O_j \phi_{P_1} |E_{0\pm},P_1\rangle , \\
M_B &= \langle O,E_{i\pm}| \sum_{j=1,3} G_{j,2} O_j \phi_{P_2} |E_{0\mp},P_2\rangle .
\end{aligned}
\tag{7}
$$

From (16) eigenvalues $\lambda_1,\lambda_2,\ldots,\lambda_6$ are derived:

$$
\begin{aligned}
&\lambda_{1,2}=\omega , \\
&\left.\begin{matrix}\lambda_{3,4}\\ \lambda_{5,6}\end{matrix}\right\} = \tfrac{1}{2}\{(\bar{\nu}_i+\omega)\pm[(\bar{\nu}_i-\omega)^2 \\
&\qquad +4(|M_A|^2+|M_B|^2)]^{1/2}\} .
\end{aligned}
\tag{8}
$$

In Fig. 13 we have plotted these vibronic energies for a specific example ($\omega=150\ \mathrm{cm}^{-1}$, $\bar{\nu}_i=140\ \mathrm{cm}^{-1}$) as a function of the interaction strength M_A ($=M_B$, assumed). We see that the fourfold degeneracy is raised and a new vibronic state ($\lambda_{3,4}$) is split off, which has mainly phonon character. Another vibronic state ($\lambda_{5,6}$) of electronic descent is repelled symmetrically to lower energies. A pure phonon state ($\lambda_{1,2}$) remains unshifted. All states are twofold degenerate. The phonon-electron hybridization of states $\lambda_{3,4}$ and $\lambda_{5,6}$ increases with the size of the matrix elements M_A,M_B: The amplitude c_3 of the electron-component in the eigenfunctions $\lambda_{3,4}$ or of the phonon component in $\lambda_{5,6}$, amounts to

$$
c_3=[1+(|M_A|^2+|M_B|^2)/(\Delta E)^2]^{-1/2} ,
$$

where ΔE is the separation between the phonon component $\lambda_{1,2}$ and the split-off vibronic state $\lambda_{3,4}$. If the interaction is strong ($\omega-\bar{\nu}_i \ll |M_A|$, $|M_B|$), $c_3\to(2)^{-1/2}$, the eigenvalues approach the asymptotic values shown as dashed lines in Fig. 13.

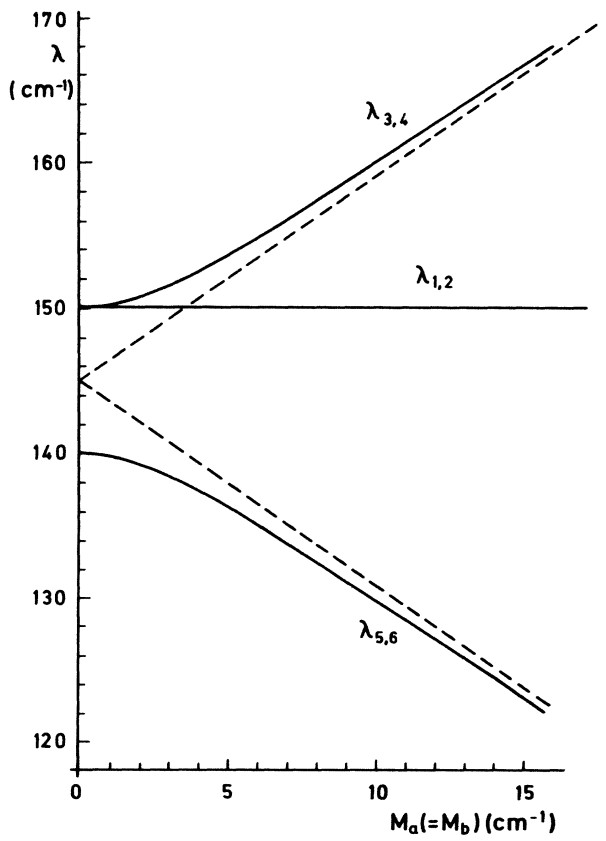

FIG. 13. Model calculation of vibronic splitting of an E phonon in a system with twofold-degenerate electronic states; the energy dependence on the coupling strength between $4f$ electrons and optical phonons is shown here.

Apparently, the spectrum becomes quite complicated in a system like CeF_3, with several E phonons close to an excited crystal-field level. Each E phonon provides one additional vibronic state and consequently shifts the energy of the interacting electronic level, while a nondegenerate phonon only causes an energy renormalization of the coupled states. Even worse, not only single-phonon states, but also many-phonon states (especially two-phonon states) close to resonance with an electronic state will interact and may gain enough intensity by hybridization to appear in the spectrum.

The remaining degeneracies will be raised, in general, by a magnetic field B along the trigonal axis because of the Zeeman-effect of the vibronic states and due to the magnetoelastic interaction[3,27,28] of the optical E phonons with the electronic levels. A (many-particle) theory, which simultaneously includes the me and vibronic interaction in a satisfying manner, does not exist at present, according to our knowledge. In order to gain some insight into the effects of a magnetic field, we formally included the me interaction into our model calculation by considering the Zeeman shift of the electronic energies $\bar{\nu}_i(B)$ in the matrix (6) and by using the phonon states corrected in second-order perturbation theory with the Hamiltonian (3) as perturbation for the calculation of the matrix elements.[28] The restriction of the product space (5) to states which are close to resonance is thus slightly released, i.e., the "polarization" of the phonon states due to electronic states not included in (6) is considered, but it

is assumed that effects of the me interaction are small as compared to the vibronic interaction. Thus supplementary elements have to be introduced into (6): the Zeeman terms additional to $\bar{\nu}_i$ and the me phonon self-energies due to (3). The largest elements of the latter type and the only ones considered here are found between the components (1,2) of a degenerate E phonon: they are of the following form:[27,28]

$$M_{1,2}(\omega)=\sum_{\substack{\alpha,N,M;\\ k,q;k',q'}} G^{\alpha,1}_{kq}G^{\alpha,2}_{k'q'}\frac{n_N-n_M}{\omega-(\bar{\nu}_M-\bar{\nu}_N)} \times\langle N\,|\,C^{\alpha,1}_{kq}\,|\,M\rangle\langle M\,|\,C^{\alpha,2}_{k'q'}\,|\,N\rangle\ , \qquad (9)$$

where $|N\rangle, |M\rangle$ are pure electronic states including $|E_{0\pm}\rangle, |E_{i\pm}\rangle$ with wave numbers $\bar{\nu}_N,\bar{\nu}_M$ and thermal occupation numbers n_N,n_M. At low temperatures, only $n_0=n(|E_{0\pm}\rangle)$ is different from zero. $\alpha,1$ or $\alpha,2$ characterizes the ir of one of the two components P_1,P_2 of the phonon in question. n_N,n_M have been introduced here *ad hoc* to reproduce the results of the theory of me effects,[28] where thermal averages have to be formed. The diagonal elements

$$M_{11}=M_{22}=\langle P_{1,2};\ldots\,|(C)^2|\,\ldots;P_{1,2}\rangle$$

give only a temperature-dependent energy renormalization[3] which is not considered here, because no qualitatively new results are provided by these terms. The off-diagonal terms, however,

$$M_{1,2}=-M^*_{2,1}=\langle P_1;\ldots\,|(C)^2|\,\ldots;P_2\rangle\ ,$$

which are purely imaginary,[30] are included and fill the hitherto open spaces in the 3×3 block matrices (6), thus lowering the symmetry of the problem. Because of n_N-n_M in (9), these matrix elements are magnetic field and temperature dependent according to

$$M_{1,2}(B)=M_{1,2}(B\rightarrow\infty)\tanh(g_I\mu_B B/k_B T)\ . \qquad (10)$$

In Fig. 14, we have plotted the results depending on B of a model calculation as in Fig. 13 for transitions starting from the lower Zeeman component of the ground state, where matrix elements of the magnetoelastic interaction $M_{1,2}$ have been introduced. Numerical values of $T=2$ K, $M_A=M_B=5$ cm^{-1}, of $|M_{1,2}(B\rightarrow\infty)|^2=25$ cm^{-2} and of $2\,\mathrm{Re}(M_{1,2}M_AM_B)=|40M_{1,2}(B)|$, have been assumed arbitrarily in addition to those values already used to calculate the plots in Fig. 13. The values $g_{x,\mathrm{I}}=1.30$ and $g_{x,\mathrm{II}}=0.45$ have been taken from Table I.

All residual degeneracies have been raised by the magnetic field. The phonon components show the typical me saturation behavior according to (1) and (10), although a small magnetic field dependence is detectable even at high fields, because of the Zeeman contribution. The splitting of the "electronic" component near 136 cm^{-1} is nonlinear and the observed g factor is different from the value entering the calculation because of the superimposed phonon splitting. At low fields ($0\le B\le1$ T) $g_{\mathrm{eff}}=1.14$ is obtained, this number decreases to $g_{\mathrm{eff}}=0.33$ at ($6\le B\le7$ T), where the splitting due to the phonon contribution has

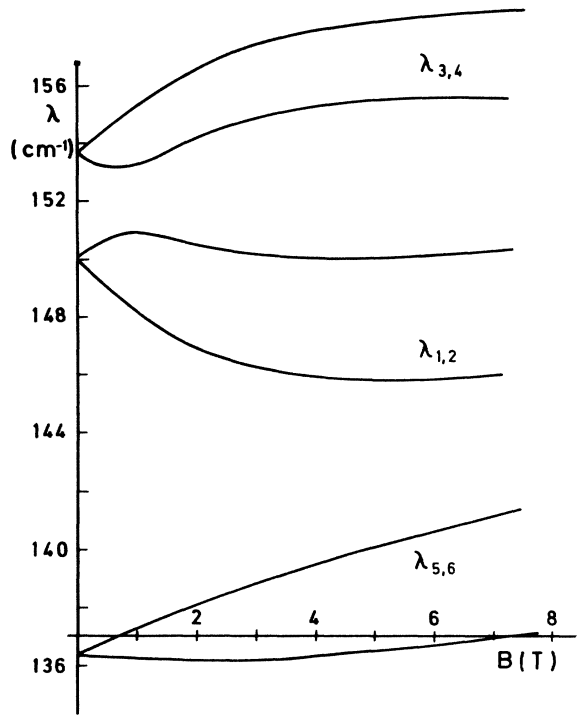

FIG. 14. Calculated magnetic field dependence of vibronic states (Fig. 13), $M_a=M_b=5$ cm^{-1}. The magnetoelastic and vibronic interactions are treated simultaneously.

saturated. The two central components of the phononlike modes demonstrate an anticrossing and an interchange of eigenvectors close to $B=1$ T, $\bar{\nu}=152$ cm^{-1}. This has the consequence that the intensities of transitions to both components of each mode may be quite different, assuming that the phonon contribution produces higher intensities in the spectrum than the electronic contribution. Thus only one component of each split mode may appear in the spectra. Line shifts nonlinear in B and saturating at high fields and intensity anomalies of the kind just described are in fact observed both in the Raman and infrared spectra of CeF_3 (Fig. 10). The complicated behavior of frequencies and intensities of phononlike vibronic state at low fields ($B<2$ T) indicated in Fig. 14 may be difficult to detect experimentally due to the large widths of the transitions involved (Fig. 6), covering finer details. With increasing magnetic field, however, these excessive widths are reduced[31] and the transitions are generally better resolved (Figs. 2, 3, and 4).

We have performed a calculation based on this model appropriate to CeF_3 which was restricted to the wavenumber regions of strong vibronic effects where the two uncoupled crystal-field states are to be expected: 170 ± 50 and 280 ± 50 cm^{-1}. All phonons within these regions were considered and coupled with the nearest electronic state. The unknown coupling constants G were treated as fit parameters. The numbers thus obtained for G are of the same size as those derived in Ref. 3 for the magnetoelastic effects. The following general results have been obtained:

(1) Some, but not all, of the additional vibronic transitions in the E spectra can be reproduced (e.g., at 300, 258, and 180 cm^{-1}, but not at 108 cm^{-1}), as well as the components with a prevailing electronic character (142 cm^{-1}).

(2) The additional transitions in the A spectra cannot be reproduced correctly. The calculations predict a coincidence of the wave numbers of A and E components, whereas significant differences are observed ($\Delta\bar{\nu} \geq 5$ cm^{-1}).

(3) All vibronic transitions should appear with the same wave numbers in the infrared and Raman spectra as predicted by this local model. This does not agree with the observations except for one, perhaps fortuitous, example.

From these facts, the conclusion has to be drawn that the local model of vibronic interaction is not fully adequate to satisfyingly interpret the experimental findings in CeF_3. It predicts correctly the existence of additional vibronic states usually not encountered in other R compounds with weak or negligible interaction, but fails to reproduce the the correct number of vibronic states and to take into account all the wave-number differences between the various types of symmetry. This failure is mostly cured by a nonlocal model of the electronic states assuming an interionic interaction within the unit cell, resulting in excitonic states with a factor-group (Davydov) splitting. There is much evidence that the dominating mechanism of this interionic interaction is again the $4f$-electron–phonon interaction (virtual-phonon exchange). A model where $4f$ excitonic states at zero wave vector are vibronically coupled to optical phonons in context with the magnetic field dependence of the infrared spectra of CeF_3 is treated elsewhere.[21] The effects of such an interionic interaction have been studied in detail, both experimentally and theoretically in PrF_3.[32]

IV. THE $4f$ GROUND STATE AND CRYSTAL-FIELD PARAMETERS IN CEF_3

In contrast to the g factors of the excited crystal-field states of $^2F_{5/2}$, the g factors of the ground state are only slightly modified by effects of vibronic interaction. Therefore, we determined the eigenvector of the electronic ground state in a manner analogous to Ref. 10, but took into consideration a horizontal axis of quantization and approximated the site symmetry by C_{2v} (orthorhombic). Thus the ground-state wave function $|q\rangle$ can be written

$$|q\rangle = u\,|\mp\tfrac{3}{2}\rangle + v\,|\pm\tfrac{1}{2}\rangle + w\,|\pm\tfrac{5}{2}\rangle\,, \tag{11}$$

with real constants u,v,w of the free-ion states $|(J=\frac{5}{2}; m_J\rangle$ and neglecting admixtures from the $J=\frac{7}{2}$ level. The following relations for the g factors are obtained:[10]

$$\begin{aligned} g_z &= \tfrac{6}{7}(-\tfrac{3}{2}u^2+\tfrac{1}{2}v^2+\tfrac{5}{2}w^2)\,, \\ 2g_x &= \tfrac{6}{7}(2\sqrt{5}uw+3v^2+4\sqrt{2}uv)\,, \\ 2g_y &= \tfrac{6}{7}(2\sqrt{5}uw+3v^2-4\sqrt{2}uv)\,. \end{aligned} \tag{12}$$

Inserting the experimental g values of Table I, three sets of solutions u_j, v_j, and w_j are obtained and given in Table II. The set $j=3$ is preferred because it comes closest to the normalization condition and it is used for all calculations of matrix elements of the magnetoelastic and vibronic interaction after multiplying u_3, v_3, and w_3 with a common factor to meet the normalization condition. Using these normalized coefficients, the following g values have been calculated: $g_x=1.57$ (1.3), $g_y=0.51$ (0.42), $g_z=0.53$ (0.48). The experimental values from Table I are given in parentheses for comparison.

TABLE II. Three possible sets of coefficients in (12) of the electronic ground state of $4f^1$ in CeF_3.

j	u_j	v_j	w_j	$u_j^2+v_j^2+w_j^2$
1	0.252	0.721	0.398	0.7411
2	0.597	0.304	0.648	0.8684
3	0.207	0.875	−0.311	0.9050

As the crystal-field splitting is approximately a factor 3 larger in CeF_3 than in $CeCl_3$,[33] it is also to be expected that the amplitudes of the contribution of $^2F_{7/2}$ states to crystal-field states derived from $^2F_{5/2}$ will increase by the same amount, from 0.1 or smaller[33] in $CeCl_3$ to approximately 0.3. This J mixing by the crystal field might account essentially for the deficiency in the normalization condition encountered with set 3 in Table II.

For the reasons mentioned in the Introduction, no direct fitting of crystal-field parameters can be performed for CeF_3. We have, however, used parameter sets given in the literature for the heavier R ions in the tysonite structure to calculate the crystal-field splitting of Ce^{3+}. Morrison and Leavitt[11] have extrapolated their results to Ce^{3+} in LaF_3; their parameters are given in column (a) of Table III. In column (b) we have compiled values taken from Dahl and Schaack[16] for Pr^{3+} in PrF_3, which have been modified to take into account the different $\langle r^k\rangle$ values ($k=2,4,6$) of $4f^2$ and $4f^1$ and the different screening factors by using the ion-dependent factors ρ_2, ρ_4, and ρ_6 tabulated in Ref. 11. In Table IV we have compiled calculated values of the crystal-field-split levels of $4f^1$ for both parameter sets using different values of the spin-orbit-coupling constant ζ. Obviously both parameter sets provide equally acceptable results with a best value of $\zeta=629$ cm^{-1} as compared to $\zeta=627$ cm^{-1} in $CeCl_3$.[33]

TABLE III. Crystal-field parameters (cm^{-1}) used to calculate the levels in Table IV. Column (a) contains parameters for LaF_3: Ce^{3+} from Morrison *et al.* (Ref. 11); column (b) contains parameters fitted to PrF_3 (Ref. 16) and adjusted to CeF_3 (Ref. 11).

B_{kq}	(a)	(b)
B_{20}	−205	−285
B_{22}	−84	−121
B_{40}	936	755
B_{42}	463+155i	379+230i
B_{44}	557+508i	537+410i
B_{60}	725	634
B_{62}	−1394−45i	−1316−70i
B_{64}	−121−732i	−26−609i
B_{66}	−669−919i	−596−827i

TABLE IV. Crystal-field levels (cm^{-1}) of the ^2F multiplet in CeF_3, calculated with the parameter sets (a) and (b) of Table III for various values of the spin-orbit-coupling constant ζ.

Parameter set	ζ (cm^{-1})	$J=\frac{5}{2}$ II	$J=\frac{5}{2}$ III	$J=\frac{7}{2}$ I	$J=\frac{7}{2}$ II	$J=\frac{7}{2}$ III	$J=\frac{7}{2}$ IV	rms deviation
(a)	623	186	306	2122	2225	2632	2894	29.3
	628.5	187	307	2142	2244	2651	2913	30.9
	643	188	308	2191	2294	2699	2960	61.6
(b)	628.5	134	306	2136	2244	2573	2842	36.9
	631	133	306	2145	2254	2582	2852	32.6
	643	134	307	2185	2293	2621	2890	35.1
Experimental values		≈ 160	≈ 280	2161	2239	2640	2860	

V. CONCLUSION

CeF_3 is an example of a R solid where the usual single-ion approximation in a static crystalline field, which has been so successful for the interpretation of a wealth of spectroscopic data over the years, fails completely, at least for the lowest electronic excitations in the range of the lattice excitations. The dynamic part of the crystalline field, i.e., the interaction between $4f$ electrons and optical phonons via the nonspherical charge distributions of the $4f$ shell in its ground state and lowest excited states, plays an important role in this material and determines the details of the energies and multiplicities of the levels both of electronic or vibrational origin. The Jahn-Teller—type interaction Hamiltonian (3), bilinear in the electronic and phonon operators, interprets the observed effects in a satisfying manner. Higher-order effects, due to products of phonon operators occurring in (3), i.e., nonlinear in the phonon displacements, have not yet been traced unambiguously in experiment (see, however, Ref. 34). It is difficult to test the theory on a quantitative basis, as in crystals of low symmetry or of complicated structure many coupling constants G are permitted by symmetry, which usually cannot be determined by fits to the few experimental data available. In a recent study of the dynamic crystal field in $LiTbF_4$ (Ref. 27) the coupling constants, i.e., the modulation of the crystalline field by optical phonons, have been calculated explicitly starting from (3) in a point-charge model, and an overall agreement of about 30% between theory and spectroscopic results has been obtained. In the view of the many approximations necessary during the course of the calculations, this result appears to be quite acceptable.

In summary, the effects of $4f$-electron—optical-phonon interaction in concentrated R compounds as treated in this paper can be classified in three categories:

If the interaction is weak, i.e., the G's are small, and phonons and crystal-field states are essentially off resonance, effects due the self-energies of phonons and electrons can be detected. This has been in fact achieved in many cases and for many R ions, most easily for the phonon system in an isomorphous series of R compounds by studying magnetoelastic effects, i.e., the magnetic phonon splitting of E mode and the zero-field temperature shift after subtracting the contribution of the anharmonic lattice: RCl_3,[35,36] RF_3,[3,37,38] and $R(OH)_3$.[39] Self-energy effects are also present in the electronic system: The resulting small wave-number shifts cannot be separated reliably from the effects of the static crystalline field and are usually not considered, even in very sophisticated model refinements during a parametrization procedure of the crystal field. g factors are a very sensitive probe and discrepancies between results obtained in careful crystal-field analyses and experimental observations have been attributed to this source.[40]

If the interaction increases or excitations close to resonance are studied, anticrossing effects with level repelling are found, i.e., an electron-phonon hybridization becomes important. This level repelling has important consequences on the electronic states: As in R compounds, the symmetry of a R site is usually lower than the point symmetry of the unit cell, and as this cell contains more than one R ion, an ir of the site group Γ_s induces several ir's of the unit-cell factor group. Thus new electronic states ("exciton states") can be constructed, originating from a level with specific site symmetry Γ_s and transforming according to the ir's of the factor group correlated with Γ_s.[41,42,32] In the absence of any interionic interaction, these states are all degenerate and there is no advantage in using the exciton model. If, however, a phonon labeled according to a specific ir of the factor group is nearby and interacts with one of these electronic substates with the correct symmetry, this and only this specific state will be repelled by the phonon, and thus the electronic degeneracy will be raised and a splitting into levels, each transforming as one of the ir of the factor group ("Davydov splitting"), will result. This Davydov splitting exists at the center of the Brillouin zone and dispersion with increasing wave vector is to be expected. Under favorable circumstances, this Davydov splitting, well known in the case of molecular crystals but due to different interaction mechanisms, can be followed experimentally to wave numbers greatly off resonance. For this case, this type of interaction has been termed "virtual-phonon exchange" and has been studied[43] in dilute systems for a long time as an interaction mechanism which becomes effective in EPR spectra of R ion pairs. Examples for Davydov splitting of crystal-field levels in the energy range of optical phonons have also been detected in PrF_3.[32,38] Other examples are currently under study.

With further increasing coupling strength the distinction between phonon and pure crystal-field states will finally lose any meaning and all states encountered have to be labeled as vibronic states, possibly with a predominant electronic or vibrational character. New states will arise in the case of Kramers degeneracy. As the selection rules for transitions between these vibronic states are different from those of pure phonon transitions, new effects will be encountered, especially in the Raman spectra (antisymmetric scattering).[24,22] CeF_3 is the only substance known to us in which all three categories apply, depending on the size of the specific coupling constants G_i related to a phonon mode i. Weak antisymmetric scattering has also been observed in PrF_3 and NdF_3,[3] but no additional vibronic transitions appeared in these substances. The magnetoelastic effects in CeF_3 have been reported earlier;[3,30] the Davydov splitting is treated in Ref. 21. The vibronic states are one of the main topics of the present work and will be considered again in Ref. 24.

It is finally of some interest to compare CeF_3 with the other important cerium halide compound $CeCl_3$. The $4f^1$-phonon coupling is stronger in CeF_3 than in $CeCl_3$. In the latter material, only magnetoelastic effects due to a weak coupling have been observed;[35] no vibronic bands appeared. The largest magnetic phonon splitting found in $CeCl_3$ amounts to 18 cm^{-1}; in CeF_3 to 28 cm^{-1}. These differences together with the different sizes of the overall crystal-field splittings may be traced back to larger interionic distances in $CeCl_3$ than in CeF_3 due to the different ionic radii of F^- (1.33 Å) and Cl^- (1.81 Å) and due to the higher symmetry of $CeCl_3$; thus the energy differences between electronic and interacting phonon states of the correct symmetry are generally larger in $CeCl_3$ than in CeF_3. It is also instructive to compare the volume per Ce^{3+} ion in $CeCl_3$, 103.7 $Å^3$, and in CeF_3, 53.0 $Å^3$.[3] Another important difference is the stronger electronegativity of the F^- as compared to the Cl^- ion. It thus appears that the extremities of each $4f^1$ wave function in CeF_3 probe a larger relative volume of the crystal than in $CeCl_3$.

At the present time, most of the new phenomena described above can only be interpreted in a qualitative manner. It is hoped that continuing efforts, both experimentally with other suitable compounds and theoretically, will contribute new insight into the different aspects of electron-phonon interaction in R solids.

ACKNOWLEDGMENTS

The authors are indebted to Dr. K. Ahrens for providing them with some of his experimental results, to Dr. W. Strobel for performing the EPR experiments, and to Dr. M. Dahl for helpful comments. The experiments at very high magnetic fields ($B > 8$ T) were performed at the Hochfeld-Magnet Labor des Max-Planck-Instituts für Festkörperforschung, Grenoble France. This work has been supported by the Deutsche Forschungsgemeinschaft (Bonn, Germany).

*Present address: Carl Zeiss, D-7082 Oberkochen, Federal Republic of Germany.

[1]A. Sher, R. Salomon, K. Lee, and M. W. Muller, Phys. Rev. **144**, 593 (1966).

[2]R. W. Waynant and P. H. Klein, Appl. Phys. Lett. **46**, 14 (1985).

[3]K. Ahrens and G. Schaack, Phys. Rev. Lett. **42**, 1488 (1979); K. Ahrens, Z. Phys. B **40**, 45 (1980).

[4]H. Gerlinger and G. Schaack, J. Phys. (Paris) Colloq. **42**, C6-499 (1981).

[5]P. Thalmeier and P. Fulde, Phys. Rev. Lett. **49**, 1588 (1982).

[6]E. Cohen and H.W. Moos, Phys. Rev. **161**, 258 (1967).

[7]F. S. Ham, in *Electronic Paramagnetic Resonance,* edited by S. Geschwind (Plenum, New York, 1972).

[8]J. H. Van Vleck and M. H. Hebb, Phys. Rev. **46**, 17 (1934).

[9]J. Becquerel, Z. Phys. **52**, 342 (1929); J. Becquerel and W. J. de Haas, *ibid.* **52**, 678 (1929); **57**, 11 (1929).

[10]J. M. Baker and R. S. Rubins, Proc. Phys. Soc. London **78**, 1353 (1961).

[11]C. A. Morrison and R. P. Leavitt, J. Chem. Phys. **71**, 2366 (1979).

[12]W. T. Carnall, H. Crosswhite, and H. M. Crosswhite, Argonne National Laboratory Report No. ANL-78, 1978 (unpublished).

[13]R. P. Bauman and S. P. S. Porto, Phys. Rev. **161**, 842 (1967).

[14]B. Maximov and H. Schulz, Acta Crystallogr. Sect. B **41**, 88 (1985).

[15]A. Zalkin and D. H. Templeton, Acta Crystallogr. Sect. B **41**, 91 (1985).

[16]M. Dahl and G. Schaack, Z. Phys. B **56**, 279 (1984).

[17]D. Gregson, C. R. A. Catlow, A. V. Chadwick, G. H. Lander, A. N. Cormack, and B. E. F. Fender, Acta Crystallogr. Sect. B **39**, 687 (1983).

[18]R. Geick and K. Strobel, in *Reviews of Infrared and Millimeter Waves,* edited by K. J. Button (Plenum, New York, 1983), Vol. 1, pp. 249–323.

[19]R. A. Buchanan, H. E. Rast, and H. H. Caspars, J. Chem. Phys. **44**, 4063 (1969).

[20]R. P. Lowndes, J. F. Parrish, and C. H. Perry, Phys. Rev. **182**, 913 (1969).

[21]H. Gerlinger, Ph.D. thesis, Universität Würzburg, 1983 (unpublished); M. Dahl, H. Gerlinger, and G. Schaack (unpublished).

[22]A. Kiel and S. P. S. Porto, J. Mol. Spectrosc. **32**, 458 (1969).

[23]C. Y. She, T. W. Broberg, L. S. Wall, and D. F. Edwards, Phys. Rev. B **6**, 1847 (1972).

[24]K. Leiteritz and G. Schaack (unpublished).

[25]V. M. T. Souza Barthem, M. Guillot, and A. Marchand, in *Proceedings of the International Conference on Magnetism, San Francisco* (ICM '85), p. 15 (unpublished).

[26]E. Gmelin, H. Grimm, and G. Schaack (unpublished).

[27]W. Dörfler and G. Schaack, Z. Phys. B **59**, 283 (1985).

[28]P. Thalmeier and P. Fulde, Z. Phys. B **26**, 323 (1977).

[29]G. F. Koster, J. O. Dimmock, R. G. Wheeler, and H. Statz, *Properties of the Thirty-two Point Groups* (MIT Press, Cambridge, 1963).

[30]K. Ahrens and G. Schaack, Indian J. Pure Appl. Phys. **16**, 311 (1978).

[31]K. Ahrens and G. Schaack, in *Proceedings of the International Conference on Lattice Dynamics,* edited by M. Balkanski (Flammarion, Paris, 1978), p. 257.

[32]M. Dahl and G. Schaack, Phys. Rev. Lett. **56**, 232 (1986).

[33]K. H. Hellwege, E. Orlich, and G. Schaack, Phys. Kondens. Mater. **4**, 196 (1965).
[34]R. J. Elliott, R. T. Harley, W. Hayes, and S. R. P. Smith, Proc. R. Soc. London, Ser. A **328**, 217 (1972).
[35]G. Schaack, Z. Phys. B **26**, 49 (1977).
[36]G. Schaack, Physica **89B**, 195 (1977).
[37]K. Leiteritz and G. Schaack, J. Raman Spectrosc. **10**, 36 (1981).
[38]M. Dahl and G. Schaack, J. Lumin. **31-32**, 84 (1984).
[39]K. Ahrens, H. Gerlinger, H. Lichtblau, G. Schaack, G. Abstreiter, and S. Mroczkowski, J. Phys. C **13**, 4545 (1980).
[40]A. Abragam and B. Bleaney, *Electron Paramagnetic Resonance of Transition Ions* (Clarendon, Oxford, 1970), p. 312.
[41]D. S. McClure, in *Solid State Physics,* edited by F. Seitz and D. Turnbull (Academic, New York, 1959), Vol. 8.
[42]R. L. Cone and R. S. Meltzer, J. Chem. Phys. **62**, 3573 (1975).
[43]J. M. Baker, Rep. Prog. Phys. **34**, 109 (1971).